2020 SNMMI Highlights Lecture: Oncology and Therapy, Part 1

Andrew M. Scott, MD, Director, Department of Molecular Imaging and Therapy, Austin Health; Head, Tumour Targeting Laboratory, Olivia Newton-John Cancer Research Institute; Professor, School of Cancer Medicine, La Trobe University; Professor, University of Melbourne; Melbourne, Australia

From the Newsline Editor: The Highlights Lecture, presented at the closing session of each SNMMI Annual Meeting, was originated and presented for more than 30 years by Henry N. Wagner, Jr., MD. Beginning in 2010, the duties of summarizing selected significant presentations at the meeting were divided annually among 4 distinguished nuclear and molecular medicine subject matter experts. Each year Newsline publishes these lectures and selected images. The 2020 Highlights Lectures were delivered on July 14 as part of the SNMMI Virtual Annual Meeting. In this issue we feature the first part of the lecture by Andrew M. Scott, MD, Director, Department of Molecular Imaging and Therapy, and Head, Tumour Targeting Laboratory, Olivia Newton-John Cancer Research Institute, Austin Health (Melbourne, Australia), who spoke on oncology highlights from the meeting. Part 2 will appear in the January 2021 issue of Newsline. Note that in the following presentation summary, numerals in brackets represent abstract numbers as published in The Journal of Nuclear Medicine *(2020;61[suppl 1]).*

It is a privilege to be able to present the oncology and therapy highlights from this year's SNMMI meeting, where a total of 509 abstracts focused on oncology topics, constituting 46% of all abstracts presented. The tracks in which these were offered covered broad areas, including Oncology: Clinical Therapy and Diagnosis (272); Oncology, Basic and Translational (102); Molecular Targeting Probes (72); Physics, Instrumentation, and Data Analysis (54); and General Clinical Specialties (9), with none in the Cardiology or Neuroscience tracks. These abstracts were submitted from a total of 34 countries, led by the United States (136), China (124), India (35), Germany (33), Japan (26), and Canada (16). It was challenging to go through all these abstracts and select those for highlighting in this summary review. I apologize to those colleagues whose excellent research and reporting I was unable to include because of time constraints.

Within this highlights talk, I will touch on several themes: novel molecular imaging probes; immuno-oncology, which remains an important focus of therapy in the oncology field; molecular imaging in treatment response assessment; imaging theranostics in prostate cancer, an area that has emerged as one of the most important for both diagnostic and therapy research; and novel therapeutics and clinical trials.

Novel Molecular Imaging Probes

Zhang et al. from Peking Union Medical College Hospital/Chinese Academy of Medical Sciences (Beijing, China), the Zentralklinik Bad Berka (Germany), Beijing Tiantan Hospital (China), and the National Institute of Biomedical Imaging and Bioengineering (Bethesda, MD) reported on "First-in-human study of a ^{64}Cu-labeled long-acting integrin $\alpha_v\beta_3$ targeting molecule ^{64}Cu-NOTA-EB-RGD in healthy volunteers and glioblastoma multiforme patients" [349]. They reported on the use of this novel imaging probe against $\alpha_v\beta_3$ in 3 healthy volunteers and 2 patients with recurrent glioblastoma. The images in Figure 1 illustrate over a 24-hour period the cumulative uptake and exquisite sensitivity and distribution of this molecule within the large area of glioblastoma in the right frontal lobe. The authors evaluated the quantitative results based on SUV in tumor compared to background and saw very high levels, confirming what was seen on the images and also in patients for whom pathology was available to assess integrin $\alpha_v\beta_3$ levels. The results indicated the safety and favorable pharmacokinetic and dosimetry profiles for this new type of PET tracer. This study highlights the ability to image $\alpha_v\beta_3$ with a PET probe. We look forward to future studies in larger cohorts of patients as this probe is explored for its potential to identify a target that can also be exploited therapeutically.

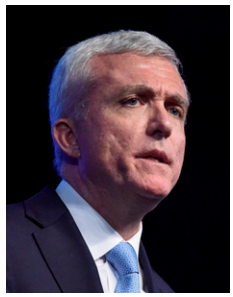

Andrew M. Scott, MD

Last year's Image of the Year at the SNMMI meeting related to imaging of fibroblast-activation protein expressed by cancer-associated fibroblasts in tumors. Chen et al. from the First Affiliated Hospital of Xiamen University (China) and the National Institutes of Health (Bethesda, MD) reported on "Comparison of ^{68}Ga-FAPI [fibroblast activation protein inhibitor] and ^{18}F-FDG PET/CT for detection, staging, and restaging of various kinds of cancer" [625] in 75 patients. Figure 2 (top) includes examples of a range of different tumor types imaged with ^{68}Ga-FAPI and ^{18}F-FDG PET, with the breast cancer example showing an especially marked increase in the number of sites of disease detected by the novel ^{68}Ga-labeled tracer. For the 75 patients evaluated, ^{68}Ga-FAPI PET had better sensitivity than ^{18}F-FDG PET for detection of lymph nodes (86.4% and 45.5%, respectively), a comparison that held for bone and visceral disease as well (83.8% and 53.5%, respectively). In the images on the bottom in Figure 2, ^{68}Ga-FAPI PET clearly demonstrated uptake in a high-grade glioma. This study is one of the first to show the difference between imaging of the tumor microenvironment and imaging of glucose metabolism in tumors. We look forward to additional research exploring this further in multicenter studies to elucidate the potential for ^{68}Ga-FAPI in identifying sites of disease and monitoring response to treatment.

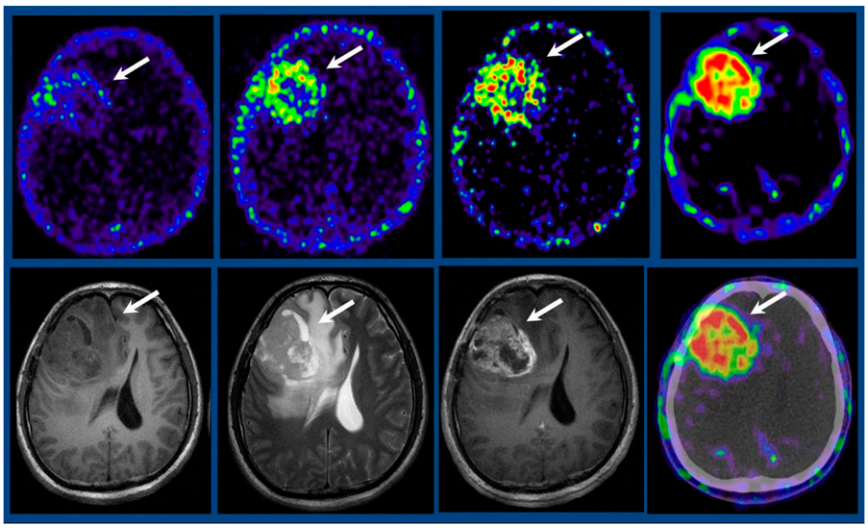

FIGURE 1. ^{64}Cu-labeled long-acting integrin $\alpha_v\beta_3$–targeting molecule ^{64}Cu-NOTA-EB-RGD in a patient with glioblastoma multiforme. Top row (left to right): ^{64}Cu-NOTA-EB-RGD PET/CT acquired at 1, 8, 12, and 24 hours after injection. Bottom row (left to right): T1-weighted MR, T2-weighted MR, T1-weighted MR with contrast, and MR + ^{64}Cu-NOTA-EB-RGD PET/CT acquired at 24 hours after injection. Images show cumulative uptake and exquisite sensitivity and distribution of this molecule within the large area of glioblastoma in the right frontal lobe and highlight the ability to image $\alpha_v\beta_3$.

In pancreatic ductal adenocarcinoma, the CCL2–CCR2 chemokine axis is used to recruit tumor-associated macrophages, which contribute to an immunosuppressive tumor microenvironment. Zhang et al. from the Mallinckrodt Institute of Radiology/Washington University School of Medicine (St. Louis, MO) reported on "PET imaging of CCR2 in pancreatic ductal adenocarcinoma" [405]. These researchers used a ^{64}Cu-DOTA-ECL1i peptide probe with which they have previously shown data in cardiac disease, as noted by Dr. Sadeghi in the Cardiovascular Highlights lecture. In this particular project they looked in a KPPC transgenic mouse model of inducible pancreatic cancer at the ability to image CCR2 expression (Fig. 3) and compared this with imaging in wild-type mice or where blocking was performed to prevent uptake from being visualized. In an example image with this probe in a patient with pancreatic cancer, CCR2 expression was seen within the pancreatic cancer. Stable tumor uptake was seen in patients with pancreatic ductal adenocarcinoma before and after chemotherapy. This was verified by histology and ~~in~~ immunohistochemistry images, where high CCR2 expression showed coexpression with CD68 macrophages. Therapeutics targeting CCR2 are currently in development, making this novel probe important as a way to image the presence of this receptor in patients who will ultimately receive such therapies.

Immuno-oncology Therapies

Immuno-oncology therapies have emerged as one of the most important and promising treatment modalities for cancer. Over the last 12 months there have been approvals of immuno-oncology drugs in non–small cell lung, small cell lung, head and neck, hepatocellular, skin, bladder, breast, esophageal, and uterine cancers. In June, we saw approval for first-line use in microsatellite instability–high or DNA mismatch repair–deficient colon cancer. Imaging of immune response and the tumor microenvironment provides important information that will assist with prognosis, prediction of response, and resistance to therapy. The 2020 American Society of Clinical Oncology (ASCO) clinical research priorities include identification of strategies that predict response and resistance to immunotherapies. In nuclear medicine we can play an important role in identifying novel probes that assist with drug development and also in appropriate selection of patients suitable for treatment as part of routine care.

^{18}F-FDG PET is used in patients who are undergoing immunotherapy, and immune checkpoint inhibitors are known for their induction of substantial toxicity. Iravani et al. from the Peter MacCallum Cancer Centre (Melbourne, Australia) reported on "FDG PET in the evaluation of immune-related hypophysitis and thyroiditis following combination ipilimumab and nivolumab in advanced melanoma" [482]. Hypophysitis is a challenging diagnosis because of the high incidence of uninterpretable biochemical assessment (due to concurrent corticosteroids) and nonspecific clinical presentation, both of which may contribute to underestimation of incidence. In a cohort of 162 patients of whom 133 had assessable PET and had received both ipilimumab and nivolumab, 31% were found to have increased uptake within the hypophysis region, which was subsequently identified through clinical as well as imaging follow-up to be related to abnormal hypophyseal function (Fig. 4). The group looked at interobserver variability and found that positive and negative predictive values were high, and with very good interobserver agreement. They also looked at thyroiditis, where the positive predictive value for subsequent biochemical abnormality was 97%. The authors concluded that ^{18}F-FDG PET detects transient increases in tracer uptake in the pituitary and thyroid gland following combined ipilimumab/nivolumab therapy, "which appears to be highly predictive of the development of these endocrinopathies, therefore prompting more stringent monitoring." They emphasized the importance of a multimodality approach in the timely diagnosis of immune-related endocrinopathies.

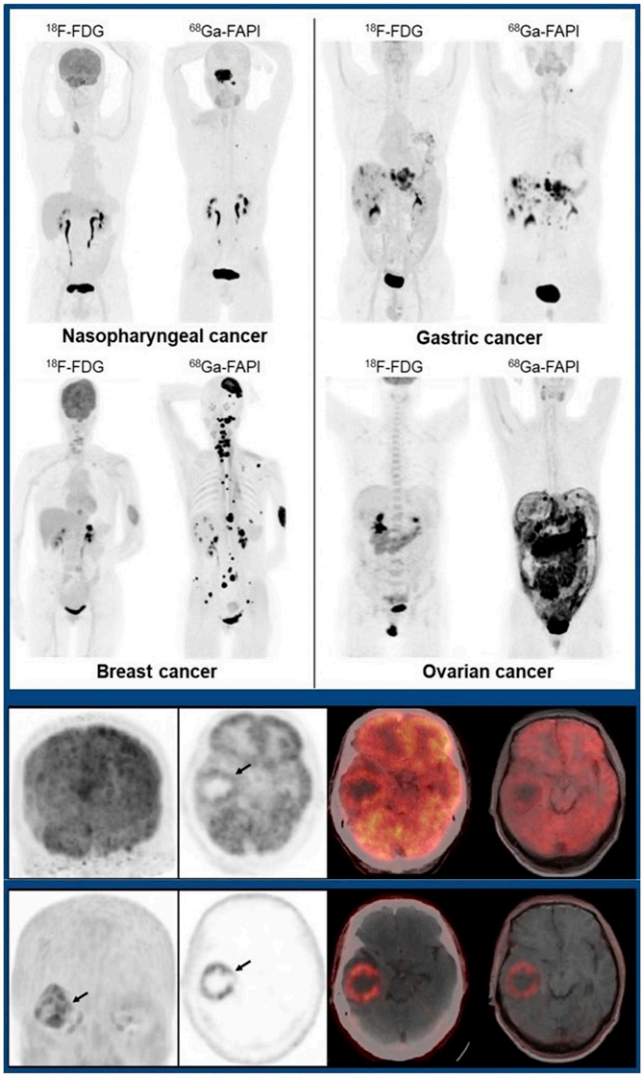

FIGURE 2. Comparison of ^{68}Ga-FAPI and ^{18}F-FDG PET/CT for detection, staging, and restaging of cancer. Top block: Example images with ^{18}F-FDG (left in each pair) and ^{68}Ga-FAPI (right in each pair) in patients with (clockwise from upper left): nasopharyngeal, gastric, ovarian, and breast cancers. Bottom block: ^{68}Ga-FAPI PET (bottom row) more clearly demonstrated a high-grade glioma and illustrated the difference between imaging of tumor marker environment and imaging of glucose metabolism with ^{18}F-labeled tracers.

Ferreira et al. from the Massachusetts General Hospital (Boston) reported on "Noninvasive detection of immunotherapy-induced adverse events" [4]. They used an elegant model to image not only immune activation but the actual T-cell activation that occurs in response to immunotherapy. In a Foxp3-GFP-DTR mouse model with syngeneic MC38 tumors they looked at a granzyme-B ^{68}Ga probe in animals treated with either phosphate-buffered saline or diphtheria toxin. Diphtheria toxin in this mouse model can substantially deplete T-reg cells. They then performed studies to determine whether the addition of anti-PD1 + anti-CTLA4 or anti-CD137 (important immune checkpoints) antibody treatment in conjunction with diphtheria toxin could induce visualization of immune activation (Fig. 5). Increased tracer uptake was seen within the liver, spleen, kidney, and bowel in these models and was reduced following dexamethasone administration. Immunofluorescent and immunohistochemical studies of colon tissue from the mice clearly showed granzyme-B expression in both cohorts treated with the immune checkpoint inhibitors. Analysis of kidney tissue samples from patients with nephritis who had been treated with immune checkpoint inhibitors showed not only upregulation of CD3 T-cell infiltrates but also granzyme-B expression in all samples tested. This granzyme-B ^{68}Ga imaging probe therefore has the potential to image the activated T-cells that occur within normal tissues as well as in tumors, and therefore may assist with prediction of potential toxicity in patients receiving immunotherapy.

Maresca et al. from Pfizer, Inc. (Cambridge, MA), Invicro (Sharon, MA), Memorial Sloan Kettering Cancer Center (New York, NY), and ImaginAb Inc. (Inglewood, CA) reported on "Preclinical evaluation of ^{89}Zr-Df-IAB22M2C PET as a potential imaging biomarker in targeted immunotherapeutic drug development of a GUCY2C-CD3 bispecific antibody PF-070621194" [408]. This study was performed in an LS1034 colon cancer model in mice, where adoptive transfer of activated T-cells was administered 1 day after treatment with this bispecific antibody. Figure 6 illustrates imaging of activated T-cells with the zirconium-labeled CD8-imaging PET probe in control (left) and treated animals (right), demonstrating that this bispecific antibody, which increases immune activation in the tumor, was associated with trafficking of CD8 cells into the tumor. Immunohistochemistry analysis of CD8+ cells confirmed higher CD8 cells in tumor in a bispecific treated mouse compared to controls. This indicates that imaging of CD8-activated T-cells can be an important way to assess the therapeutic efficacy of immunotherapy aimed at increasing tumor-infiltrating T-cells. The authors concluded that their ^{89}Zr-Df-IAB22M2C PET agent "shows potential as an imaging biomarker for immune activation measurement to assess the proof-of-mechanism for potential future clinical application in the assessment of CD8 T-cell recruitment." I congratulate the authors on this important study.

Nobashi et al. from Stanford University School of Medicine/Stanford University (CA) reported results of an elegant study on "Imaging-activated immune response following therapeutic vaccination in an orthotopic glioma model with ^{89}Zr-DFO-OX40 monoclonal antibody PET" [2]. They used syngeneic GL261 cells injected into the brains of mice in this model to look at the ability of an OX40 antibody labeled with ^{89}Zr to image activated CD4+ T-cells. They also looked at vaccination, where they used a combination of an adjuvant CpG in conjunction with GL261 cells and OX40 monoclonal antibody to determine

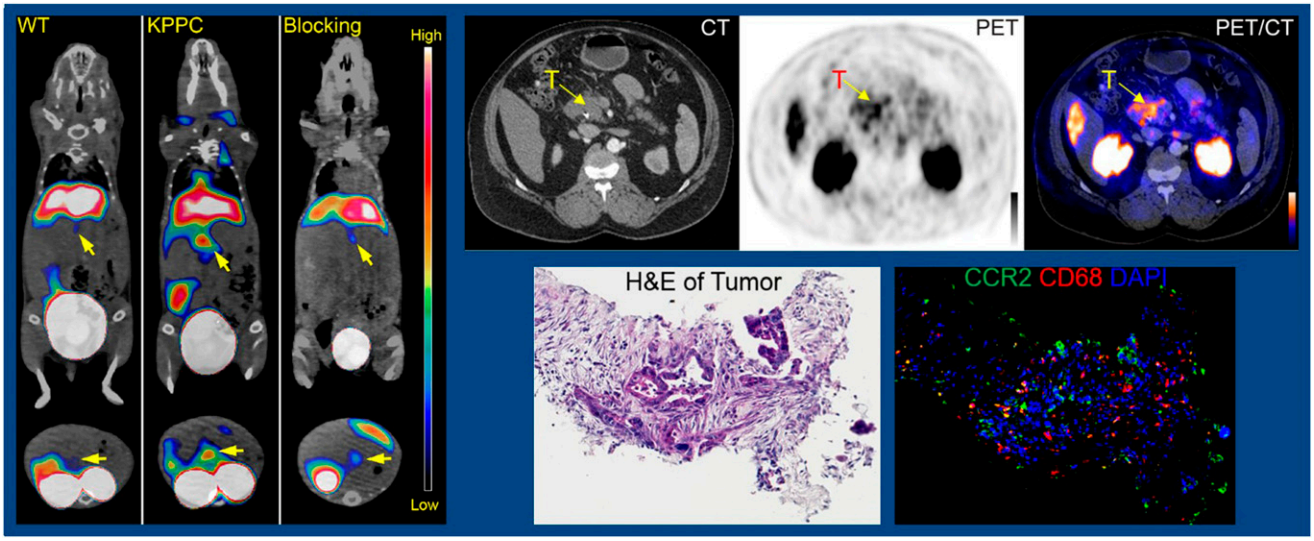

FIGURE 3. ^{64}Cu-DOTA-ECL1i PET imaging of CCR2 in pancreatic ductal adenocarcinoma (PDA). Left block (left to right): Imaging in wild-type mouse, a KPPC transgenic mouse model of inducible PDA, and with blocking. Right (top, left to right): CT, ^{64}Cu-DOTA-ECL1i PET, and ^{64}Cu-DOTA-ECL1i PET/CT imaging in a patient with PDA, showing CCR2 expression within the pancreatic cancer. Right (bottom): This was verified at histology (left) and in immunohistochemistry (right), where high CCR2 expression showed coexpression with CD68 macrophages.

whether they could reduce the size of the tumor and use PET/CT to evaluate the associated impact on distribution of OX40 expression. On the right in Figure 7 is a control mouse, where the glioma is present in the brain and OX40 imaging shows only distribution within blood pool and (to some degree) catabolism in liver and spleen. However, in the vaccinated mice (left) with an increased CD4 T-cell presence both in vaccinated and tumor-draining lymph nodes, the researchers were able to clearly visualize activation of the immune system and trafficking of CD4 cells. This is a very important observation, because it highlights the fact that the intrinsic components of the immune system can be imaged with PET to dynamically guide assessment of immune response to new immunotherapy approaches, including vaccine strategies targeting glioma.

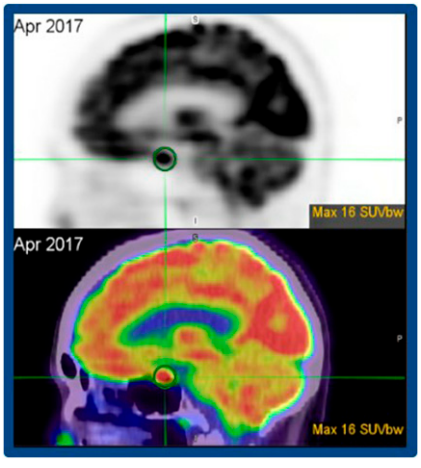

FIGURE 4. ^{18}F-FDG PET in evaluation of immune-related hypophysitis and thyroiditis following combination ipilimumab and nivolumab in advanced melanoma. Example PET (top) and PET/CT (bottom) imaging shows increased uptake within the hypophysis region, which was subsequently identified in many patients to be related to abnormal hypophyseal function.

Molecular Imaging in Treatment Response Assessment

We know that different tumor types have varying pathologic and metabolic responses to treatment, and that we can use nuclear medicine imaging studies to assess response in a systematic and accurate way. We also know that different treatment approaches have different response characteristics. This is exemplified in the study by Tatsumi et al. from Osaka University Graduate School of Medicine and JAPAN Suita (both in Osaka, Japan), who reported on "Prediction of chemotherapeutic response with volumetric parameters or texture features on FDG PET in recurrent gynecological malignancies" [355]. They explored whether volumetric parameters (metabolic tumor volume and total lesion glycolysis) or texture features on baseline ^{18}F-FDG PET were useful in predicting treatment response after 1 cycle of chemotherapy in 25 patients. They found that entropy (a texture feature) as assessed at baseline was predictive of response after the first chemotherapy cycle (Fig. 8). Volumetric parameters, however, were more useful than texture features in predicting final treatment response. This is an interesting study, because it illustrates how texture features from ^{18}F-FDG PET can be used in addition to volumetric parameters to assist with identifying patients who might respond better to treatment. This will be explored in additional studies and holds promise for a number of other oncology indications.

Some years ago, as we were embarking on assessment of patients receiving new cancer therapeutics, it became clear that we would need to develop an improved way to assess and compare ^{18}F-FDG PET imaging results. The PET Response Criteria in Solid Tumors (PERCIST) were

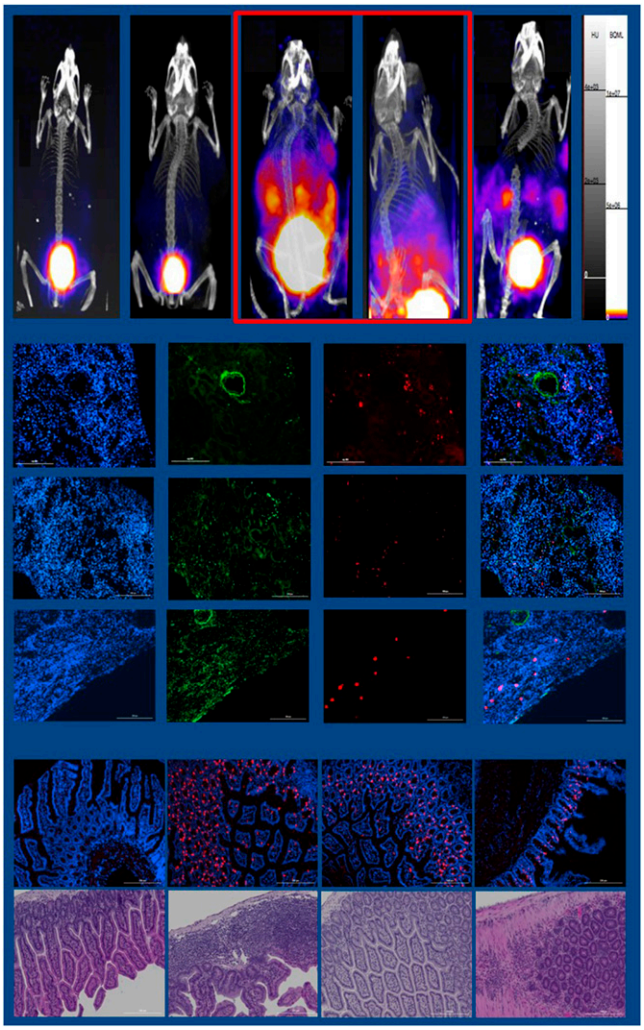

FIGURE 5. Noninvasive detection of immunotherapy-induced adverse events. Top block: ^{68}Ga-NOTA-GZP imaging in a Foxp3-GFP-DTR mouse model with syngeneic MC38 tumors treated with (left to right): phosphate-buffered saline, diphtheria toxin, diphtheria toxin + anti-CD137, diphtheria toxin + anti-PD1 + anti-CTLA4, and diphtheria toxin + anti-CD137 + dexamethasone. Red outline indicates induction of adverse events. Middle block: Stained kidney tissue samples (left to right: DAPI fluorescent, CD3, granzyme B, and 3-stain merge) from patients presenting with checkpoint inhibitor–associated nephritis. Not only upregulation of CD3 T-cell infiltrates but also granzyme-B expression were found in all samples tested. Bottom block: Immunofluorescence (top) and H&E (bottom) analyses of tissue from mice treated with (left to right) phosphate-buffered saline, diphtheria toxin + anti-CD137, diphtheria toxin + anti-PD1 + anti-CTLA4, and diphtheria toxin + anti-CD137 + dexamethasone. Red staining by immunofluorescence indicates granzyme B, demonstrating activation of T-cells following treatment, which was reduced by dexamethasone.

established by Richard Wahl, MD, and colleagues. At this year's SNMMI meeting, Mhlanga et al. (with Dr. Wahl as senior author) from the Mallinckrodt Institute of Radiology/Washington University in St. Louis (MO) reported on a "Systematic review of the utilization of PERCIST 1.0 metabolic response criteria in prospective clinical trials" [128]. They reviewed the literature and identified 73 prospective trials in which PERCIST was utilized in a total of 2,807 patients. Only 56 of the studies reported survival data, with 38 of these (68%) reporting overall survival. Of these, PERCIST was reported to be predictive of overall survival in 71%. Twenty-eight of the 56 studies reported on progression-free survival, for which PERCIST was predictive in 71.4%. In no instance was a favorable response on PERCIST 1.0 (complete response, partial response, stable disease) associated with less favorable outcomes than progressive disease on PERCIST 1.0. The ability to apply these types of criteria in a consistent and standardized manner is essential if we are to properly analyze this approach in future trials. The authors concluded that "Prospective inclusion of the PERCIST 1.0 criteria in clinical trials using FDG, with baseline, early monitoring, and end-of-therapy scans could inform cancer clinical trials." I agree and support the use of PERCIST in a standardized manner at these timepoints to inform cancer clinical trials moving forward.

Wang et al. from the University of California Davis (Sacramento) and Imperial College London (UK) shared at this meeting a number of reports on total-body PET using the EXPLORER system. In one of these presentations, they reported on "Total-body dynamic PET of metastatic cancer: First patient results" [208]. They showed high-quality ^{18}F-FDG parametric images of metastatic cancer. Figure 9 is an example of a patient with metastatic kidney cancer serially imaged over a 1-h period. We are only at the beginning of exploring the extraordinary potential of this very sophisticated approach performing total-body kinetic modeling and generating dynamic parametric data that can be used with a variety of imaging probes in patients with cancer. We look forward to seeing this applied with new tracers moving forward and congratulate again this group on this transformative new technology.

Prostate Cancer: Imaging

Prostate cancer is an area that has been transformed through nuclear medicine imaging and therapies, particularly over the last 5 years. At this year's SNMMI meeting we saw again very impressive presentations from groups from around the world looking at a range of imaging PET probes. More important, we saw the results of large multicenter trials exploring initial staging in high-risk disease, staging following biochemical relapse, and management impact. As we look at data from these and ongoing studies, it is crucial to continue to consider competing modalities (e.g., conventional imaging, multiparametric MR imaging) for staging investigations in comparison to and in combination with PET studies. The increasing volume of clinical results and health economic analyses should support more regulatory and funding approvals in this area. I am delighted to be able to present some highlights from the prostate cancer imaging studies presented at the SNMMI meeting.

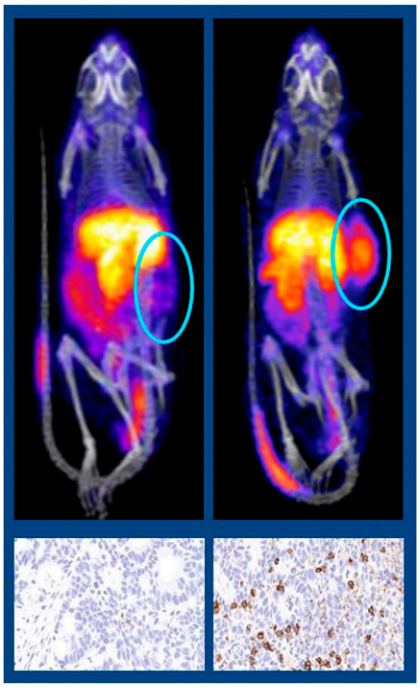

FIGURE 6. ^{89}Zr-Df-IAB22M2C PET as a potential imaging biomarker in targeted immunotherapeutic drug development of GUCY2C-CD3 bispecific antibody PF-070621194. Zirconium-labeled CD8 PET/CT and corresponding immunohistochemical analysis in an LS1034 adoptive transfer colon cancer model showed activated T-cells in tumor (circle) in antibody-treated (right) but not isotype control-treated (left) animals, demonstrating that this bispecific antibody was associated with trafficking of CD8 cells into the tumor.

The first of these was a summary of results from the CONDOR study, a large, prospective multicenter trial in the United States and Canada. Rowe et al. from the Johns Hopkins School of Medicine (Baltimore, MD), Yale University School of Medicine (New Haven, CT), CHU de Quebec/Laval University Quebec (Canada), Tower Urology (Los Angeles, CA), the University of California at San Francisco, City of Hope (Sierra Madre, CA), Hospital of the University of Pennsylvania (Philadelphia), University of Michigan (Ann Arbor), H. Lee Moffitt Cancer Center and Research Institute (Tampa, FL), the University of Wisconsin Madison, Stanford University (CA), University of Iowa Hospital (Iowa City), Progenics Pharmaceuticals, Inc. (New York, NY), Memorial Sloan Kettering Cancer Center (New York, NY), and Washington University School of Medicine (St. Louis, MO) reported on "Diagnostic performance of prostate-specific membrane antigen (PSMA)–targeted ^{18}F-DCFPyL PET/CT in men with biochemically recurrent prostate cancer: Results from the phase 3, multicenter CONDOR study" [38]. A total of 207 patients have been enrolled in the study and were required to have an increase in prostate-specific antigen (PSA) levels after definitive prostate cancer therapy but negative or equivocal imaging by standard workup, no ongoing systemic therapy, and no treatment with androgen deprivation therapy in the 3 months prior to administration of the PET tracer. The study used central blinded independent readers to assess the results of the scans. They applied a correct localization rate, which was defined by the FDA as the percentage of patients with a 1-to-1 correspondence between localization of at least 1 lesion identified by ^{18}F-DCFPyL PET/CT and a composite standard of truth, which could be subsequent histopathology, conventional imaging, or a post-treatment PSA change for irradiated lesions. They found a correct localization rate of between 84.8% and 87% for the 3 independent readers. This easily achieved the primary endpoint of a lower limit of the 95% confidence interval for the correct localization rate exceeding 20% for 2 of the 3 readers. This is an important and practice-changing study, because it validates the excellent diagnostic performance of ^{18}F-DCFPyL in patients with biochemically relapsed prostate cancer, even at low PSA values. Another presentation on this trial was given at the ASCO meeting

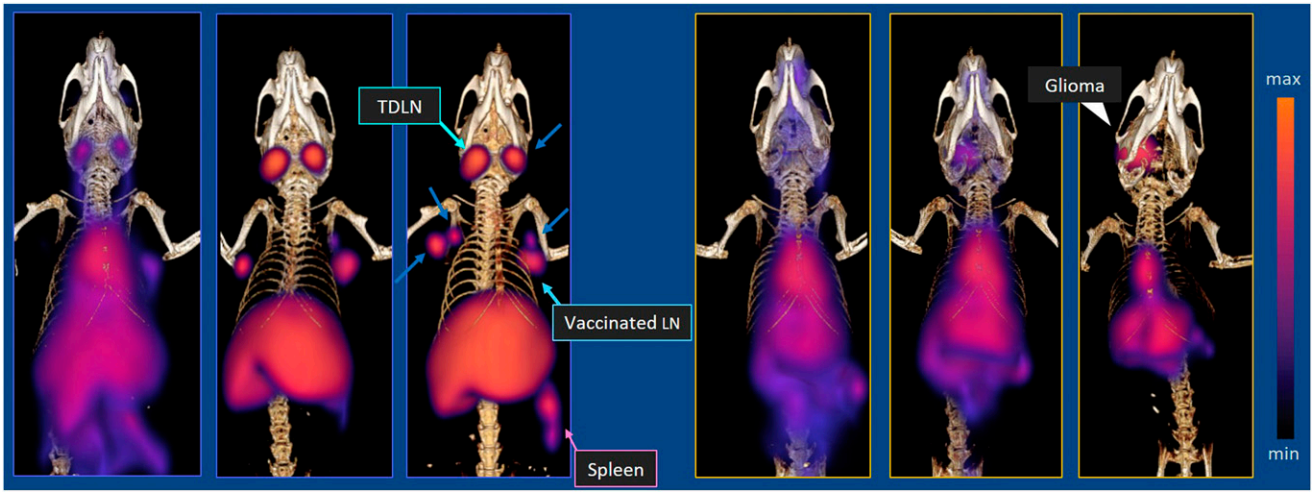

FIGURE 7. ^{89}Zr-DFO-OX40 monoclonal antibody PET imaging of immune response in an orthotopic glioma model (left 3 images) at days 1, 2, and 5 following therapeutic vaccination and (right 3 images) at corresponding days in an unvaccinated control. ^{89}Zr-DFO-OX40 mAb PET visualized activation of the systemic immune responses triggered by therapeutic vaccination, highlighting the translational potential of this approach to monitor T-cell activation in vaccine strategies targeting glioblastoma.

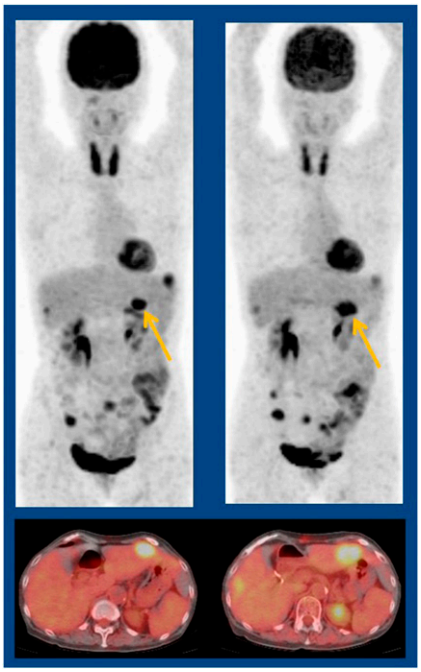

FIGURE 8. ^{18}F-FDG PET volumetric parameters and texture features in prediction of response to chemotherapy in recurrent gynecologic malignancies. PET and PET/CT imaging in an example patient with ovarian cancer before treatment (left: SUV_{max} = 6.7; metabolic tumor volume [MTV] = 7.4; entropy = 4.3) and after 1 cycle of chemotherapy (right: SUV_{max} = 5.5; MTV = 15.6). Entropy (a texture feature) as assessed at baseline was predictive of nonresponse after the first chemotherapy cycle. Changes in volumetric parameters (MTV, total lesion glycolysis, and SUV_{max}) assessed pre- and post-1 cycle of chemotherapy were useful in predicting final treatment response.

in early June, where Morris et al. presented data on changes in management resulting from ^{18}F-DCFPyL PET/CT in the study. Among evaluable patients, 63.9% had changes in intended management, ranging from noncurative therapy to salvage therapy (or vice versa) or observation to initiation of therapy (or vice versa). I congratulate the authors of these abstracts and all those involved with the CONDOR study. We are delighted that it was presented at the SNMMI meeting this year.

Another relevant and influential recent study not presented at this SNMMI meeting was from Hofman et al. from 10 sites in Australia and was published in *The Lancet* (2020;395:1208–1216): "PSMA PET-CT in patients with high-risk prostate cancer before curative-intent surgery or radiotherapy (pro-PSMA): A prospective, randomized, multicentre study." Unlike other studies that have looked at biochemical relapse of prostate cancer, this group focused on a patient population with untreated but biopsied and proven prostate cancer who were at high risk (high PSA values, Gleason grade group 3–5, or clinical stage ≥T3). The study included 302 patients who were randomized to first-line imaging with either conventional CT and bone scan or to ^{68}GA-PSMA-11 PET/CT within 3 weeks of randomization. All patients who were not found to have multiple metastases were then crossed over to imaging with the other modality. A total of 282 patients underwent imaging with both approaches, with 6-month follow-up and a composite standard of truth to assess accuracy. ^{68}Ga-PSMA-11 PET/CT was found to have significantly greater accuracy than standard imaging with CT or bone scan (92% and 65%, respectively; $P < 0.001$). A change in management occurred in 28% of PSMA-imaged patients compared to 15% of conventionally imaged patients. The authors concluded that "PSMA PET-CT is a suitable replacement for conventional imaging, providing superior accuracy, to the combined findings of CT and bone scanning." These findings are practice changing and illustrate the role of nuclear medicine imaging in early-diagnosed, high-risk prostate cancer patients. From initial diagnosis through the spectrum of progression of disease, imaging with nuclear medicine probes plays a significant role in prostate cancer.

Ferdinandus et al. from University Hospital Essen (Germany), the University of California Los Angeles, the Technische Universität München (Germany), and the University of California San Francisco reported on the "Impact of ^{68}Ga-PSMA-11 PET on management of recurrent prostate cancer in a prospective single-arm clinical trial" [43]. In this study of patients with biochemical recurrence, the researchers found a 68% (260/382) change in intended management, with 46% (176/382) considered major changes. A total of at least 150 intended diagnostic tests were avoided,

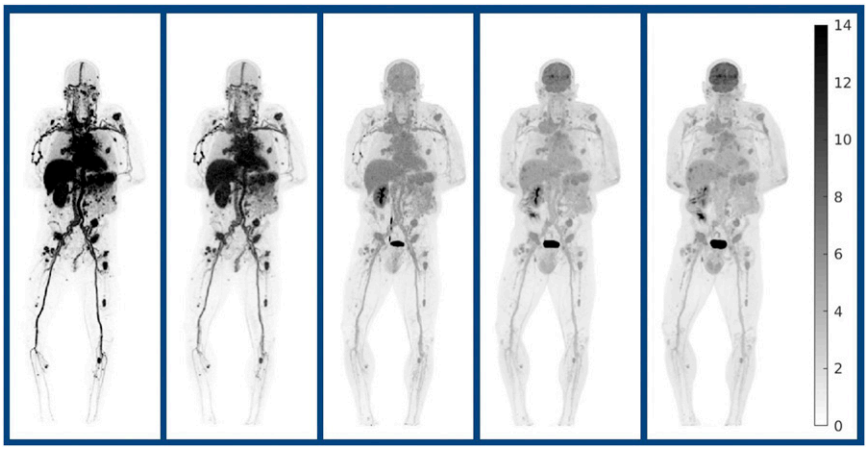

FIGURE 9. Total-body dynamic parametric ^{18}F-FDG PET images in a patient with metastatic kidney cancer scanned on the uEXPLORER at (left to right): 0.5–1, 1–2, 10–12, 30–35, and 55–60 minutes after injection.

FIGURE 10. ^{18}F-DCFPyL PET/CT image in a patient with suspected limited recurrent prostate cancer after primary therapy. A new lesion was identified on ^{18}F-DCFPyL PET/CT that was not seen on conventional imaging.

and the percentage of patients with unknown sites of disease declined from 68% to 29%. The predominant management changes were in line with the ^{68}Ga-PSMA-11 PET stages: changes toward active surveillance (47%) for unknown disease sites, toward local/focal therapy (56%) for locoregional disease, and toward systemic therapy (69% M1a; 43% M1b/c) for metastatic disease. These results clearly show the clinical impact of PSMA PET imaging in prostate cancer patients with biochemical relapse.

Another large multicenter study came from Metser et al., from the University of Toronto, McMaster University (Ancaster and Hamilton), Western University (London), and Cancer Care Ontario (Toronto; all in Canada), who reported on "Preliminary results of a prospective, multicenter trial assessing the impact of ^{18}F-DCFPyL PET/CT on the management of patients with recurrent prostate cancer" [40]. Participants had suspected limited recurrent disease, with biochemical failure and no or ≤4 sites of disease after primary therapy. Of a total of 410 men, 261 (64%) had ^{18}F-DCFPyL PET/CT–detected lesions (Fig. 10 shows example image). More than half of patients (56%) with negative conventional imaging were found to have positive sites on PET/CT. Even among men with lesions identified on conventional imaging, >60% had new lesions identified on PET/CT, ranging from local and regional disease to more distant metastases. Of note, post-PSMA imaging management changes were reported in 341 of the 410 patients, with 66% of these determined to be PET/CT directed. Long-term follow-up is needed to evaluate the impact on disease control. It appears, then, that whatever PSMA imaging probe is used in patient populations with suspected recurrent disease and biochemical relapse, up to 2/3 will routinely have management changes as a result of PET imaging.

One of the other interesting PSMA probes developed over the last few years is PSMA-7. Rauscher et al. from the Technische Universität München (Germany) and the Klinikum Rechts der Isar (Munich, Germany) reported on "Matched-pair comparison of ^{68}Ga-PSMA-11 and ^{18}F-rhPSMA-7 PET/CT in patients with primary and biochemical recurrent prostate cancer" [42]. This retrospective analysis included 160 patients who had undergone ^{18}F-rhPSMA-7 PET/CT and 160 patients who had undergone ^{68}Ga-PSMA-11 PET/CT. These were separate cohorts matched for patient characteristics rather than patients who underwent both studies. The tumor positivity rate was found to be consistently high for both tracers. A number of areas of uptake for both tracers were reliably identified by trained physicians as benign (e.g., ganglia, nonspecific lymph node uptake, and even fibro-osseous lesions) (Fig. 11). Of interest, the number of sites of benign uptake was much higher with ^{18}F-rhPSMA-7 than with ^{68}Ga-PSMA-11, which the authors speculate could be the result of the improved PET resolution of ^{18}F and therefore a characteristic common to many novel ^{18}F-labeled agents. Again, it is important to be able to recognize patterns of normal tissue uptake when interpreting PSMA PET scans.

Akintayo et al. from Emory University and the Rollins School of Public Health (Atlanta, GA) reported on "^{18}F-fluciclovine PET/CT versus multiparametric MRI assessment of seminal vesicle invasion and extracapsular extension in patients with primary prostate cancer" [1243]. They evaluated 35 newly diagnosed patients with prostate cancer to assess seminal vesicle infiltration and extracapsular extension,

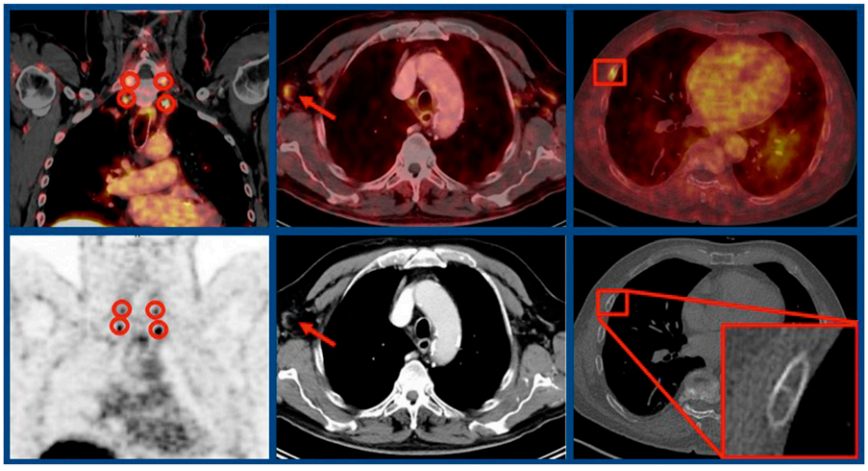

FIGURE 11. Comparative imaging with ^{18}F-rhPSMA-7 PET/CT and PET in cervical ganglia (left); ^{68}Ga-PSMA-11 PET/CT and CT in an unspecific axillary lymph node (middle); and ^{18}F-rhPSMA-7 PET/CT and PET CT in a fibro-osseous lesion (right) in patients with primary and biochemical recurrence of prostate cancer.

and compared ^{18}F-fluciclovine PET/CT with multiparametric MR imaging, which is the standard usually employed by surgeons and oncologists to assess local extension of prostate cancer at original diagnosis. The authors found that ^{18}F-fluciclovine PET had a higher sensitivity (68.8% vs 37.5%) but a lower specificity (57.9% vs. 87.5%) than multiparametric MR imaging for seminal vesicle infiltration; these results held true for evaluation of extracapsular extension (48.3% vs 44.3% and 83.3% vs 100%, respectively) (Fig. 12). They concluded that there does not appear to be a significant difference between the ability of ^{18}F-fluciclovine PET/CT and multiparametric MR imaging in local staging of prostate cancer in newly diagnosed patients with high-risk prostate cancer. This was a challenging study to perform and provides important information that allows us to more appropriately reconcile the relative roles of imaging approaches in locally advanced prostate cancer at initial diagnosis.

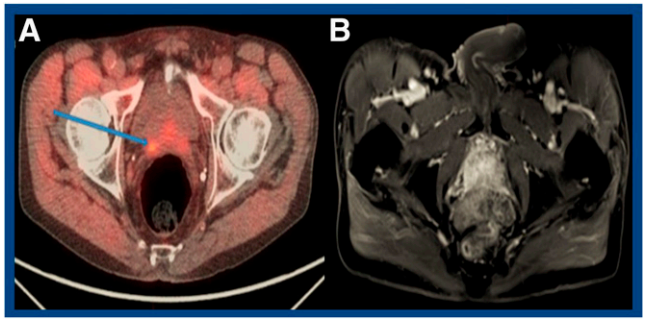

FIGURE 12. ^{18}F-fluciclovine PET/CT versus multiparametric MR imaging assessment of seminal vesicle invasion and extracapsular extension in primary prostate cancer. Example image in a 65-year-old man with primary prostate cancer (PSA = 47.92 ng/mL, Gleason score = 4.3). ^{18}F-fluciclovine PET/CT (A) showed abnormal uptake in right seminal vesicle suggestive of invasion (blue arrow), whereas MR imaging (B) reported no evidence of seminal vesicle invasion. Histology confirmed right seminal vesicle invasion.

SNMMI Bylaws Committee Notice to the Membership

The SNMMI Bylaws Committee met in virtual video session on October 13, 2020, and approved several proposed amendments to the bylaws. In accordance with requirements for amending the bylaws, the proposed amendments are published herein. The amendments will be voted on by the House of Delegates during its virtual meeting, which will coincide with the SNMMI Mid-Winter Meeting in January 2021.

The amendments fall into 2 groups. The first would modify the election of Directors-at-Large to the Board of Directors. The SNMMI Task Force on Diversity, Equity, and Inclusion has recommended that a pathway be developed that would allow candidates for Director-at-Large positions to be selected from among qualified members in the general membership. This option would provide a pathway for members of underrepresented groups (as defined by the Association of American Medical Colleges) to enter SNMMI leadership without being members of the House of Delegates. (Voting members of the House comprise delegates from Chapters, Councils, Centers, and the Technologist Section, as well as the SNMMI Historian.) At present the House of Delegates elects 4 Directors-at-Large from among its membership (excluding Technologist delegates). The proposed amendments provide for election of 2 Directors from among the full members of the Society and 2 Directors from among members of the House. The election of 3 Directors-at-Large by the Technologist Section is not changed by these amendments.

The second group of amendments includes housekeeping items that correct minor inconsistencies or errors and provide more consistent wording.

Submitted on behalf of the Bylaws Committee by:
James M. Woolfenden, MD
Chair

Proposed Amendments to the SNMMI Bylaws

ARTICLE III MEMBERSHIP; Section 3: DISCIPLINE

B. The Committee on Ethics shall review, either on its own initiative or on written and signed complaint, any case in which the circumstances in Section~~s~~ 3:A ~~or 4:A~~ may lead to potential discipline and shall forward to the House of Delegates any recommendation on possible action. Such review shall afford the accused member an opportunity for a hearing.

ARTICLE VII HOUSE OF DELEGATES; Section 2: RESPONSIBILITIES

A. To develop and recommend to the Board of Directors, Society policies and programs regarding professional issues affecting nuclear medicine and molecular imaging.
B. To elect ~~the seven (7)~~ two (2) Directors-at-Large~~, the majority of the voting members of the Board of Directors.~~
C. To approve amendments to the Bylaws in accordance with the Bylaws and Procedures.

(Continued on page 40N)

D. To approve establishment, suspension, renewal and dissolution of chapters and councils.
E. To review the strategic plan annually.
F. To oversee and monitor the work of the committees of the House of Delegates.
G. To elect the Vice-Speaker of the House (who ascends to speaker), and the Historian.
H. To elect the members-at-large of the Committee on Nominations.
I. To elect the members of the Audit Committee.
J. To approve the selection of the Editor of *The Journal of Nuclear Medicine.*

ARTICLE VIII ELECTIONS; Section 2: COMMITTEE ON NOMINATIONS

A. The Committee on Nominations shall consist of a Chair plus six additional members. The House of Delegates at the Annual Meeting shall elect the members of the committee, except the Chair, from among those who will continue to serve as voting members in the House the following year.
B. The Committee on Nominations shall be chaired by the Past President–once-removed, who shall vote only in the case of a tie vote on the committee. If the Past President–once-removed is not able to serve, the next more senior available Past President shall chair the committee.
C. The term of the Committee on Nominations shall commence at the conclusion of the Annual Meeting at which it is elected and shall terminate at the conclusion of the next Annual Meeting.
D. The Committee on Nominations will solicit, verify, and submit to the membership ~~a slate of~~ candidates for Society Officers and two (2) Directors-at-Large.
E. The Committee on Nominations shall solicit, verify, and submit to the House of Delegates ~~a slate of~~ candidates for Vice-Speaker of the House, Historian, and two (2) Directors-at-Large (other than Directors-at-Large chosen by the Technologist Section).

ARTICLE X BOARD OF DIRECTORS; Section 3: COMPOSITION

The Board of Directors shall be composed of fifteen (15) voting members and six (6) non-voting members.

A. Voting Members
1. Society Officers: President, Vice President, Vice President-Elect, and the Secretary/Treasurer. The President shall serve as Chair of the Board of Directors.
2. Immediate Past President
3. President of the Technologist Section
4. Immediate Past President of the Technologist Section
5. Speaker of the House of Delegates
6. Seven (7) Directors-at-Large
   a) Directors-at-Large shall serve for a three (3)-year term, which shall commence at the conclusion of the Annual Meeting at which they are elected and which shall terminate at the conclusion of the third subsequent Annual Meeting following the election. A Director-at-Large chosen by the Technologist Section may serve for a term of less than three years at the discretion of the Technologist Section. Directors-at-Large may serve no more than two (2) consecutive terms, following which at least three years must elapse before service as a Director-at-Large is again permitted.
   b) Candidates for Director-at-Large must have been a member of the Society for at least three (3) years to be eligible to serve on the Board of Directors.
   c) ~~Four (4)~~ Two (2) Directors-at-Large shall be elected by the House of Delegates from among the voting Delegates of the House.
   d) Two (2) Directors-at-Large shall be elected from among the Full members who are not House members or Technologist Section members.
   e) Three (3) Directors-at-Large shall be elected by the Technologist Section from among the eight (8) Technologist Section Delegates of the House in accordance with procedures established by the Technologist Section.